Journal of Petroleum Exploration and Production Technology (2024) 14:2257–2272
https://doi.org/10.1007/s13202-024-01823-6

ORIGINAL PAPER-PRODUCTION ENGINEERING

Application of artificial intelligence to predict rock strength and drilling efficiency using in-cutter sensing data and vibration modes

Alexis Koulidis[1] · **Guang Ooi**[1] · **Shehab Ahmed**[1]

Received: 15 November 2023 / Accepted: 14 May 2024 / Published online: 30 May 2024

Abstract
Drilling is a complex destructive action that induces vibrations due to the rock-bit interaction, which affects the overall drilling efficiency and wellbore quality. This study aims to enhance drilling efficiency by deploying artificial neural networks (ANNs) to integrate in-cutter force sensing and vibration data. Data is collected from experiments conducted with sharp cutters on rock samples of varying mechanical properties, measuring variables such as weight on bit, torque, rotational speed, in-cutter force, and vibration measurements. A scoring system is used to evaluate the drilling efficiency by coupling the mechanical specific energy and vibration modes. An ANN is trained with these variables to predict the rate of penetration and rock strength, which are also measured in the experiments to be used as ground truth. The reliability of the framework is demonstrated by testing the validity of the ANN model on samples with various mechanical properties. It introduces a reliable and swift method for determining optimal drilling parameters, supported by a sensitivity analysis to fine-tune the ANN and assess the influence of each parameter on performance. This study demonstrates that ANN could be successfully implemented to predict the rate of penetration and rock strength on a laboratory-scaled drilling rig. The results show that the ANN model accurately predicts training and testing datasets for scoring while drilling multiple layers with a correlation coefficient of 0.966. Integration of in-cutter sensing technology, vibration data, and ANN can be of significant interest and be used on field applications to provide a reliable and rapid decision about drilling efficiency.

Keywords In-cutter sensing · Artificial neural network · Rock strength · Drilling efficiency

List of symbols

Latin symbols

A	Cutting area [mm^2]
DOC	Depth of cut [mm]
F_n	Normal force [N]
F_s	Force perpendicular to cutter's face [N]
F_t	Tangential force [N]
MSE	Mechanical specific energy [MPa]
RPM	Revolutions per minute
TOB	Torque on bit [Nm]
UCS	Uniaxial compressive strength [MPa]
ROP	Rate of penetration [mm/s]
WOB	Weight on bit [N]
$RMSE$	Root mean square error
$AAPE$	Average absolute percentage
RMS	Root mean square

Greek symbols

ϵ	Intrinsic specific energy [MPa]
χ_{est}	Estimated/predicted value
χ_{exp}	Expected value

Abbreviations

ANN	Artificial neural network
ML	Machine learning

Guang Ooi and Shehab Ahmed have contributed equally to this work.

✉ Alexis Koulidis
alexis.koulidis@kaust.edu.sa

Guang Ooi
guang.ooi@kaust.edu.sa

Shehab Ahmed
shehab.ahmed@kaust.edu.sa

[1] Physical Science and Engineering Division, King Abdullah University of Science and Technology, 23955 Thuwal, Saudi Arabia

Introduction

Drilling optimization has been the primary focus of research for the past 70 years, with the initial research focusing on the effect of surface parameters, including weight on bit (WOB) and rotational speed (RPM) to the rate of penetration (Speer 1959). The effect of rotary speed seems to be more complex and is a function of bit life (Wardlaw Wardlaw 1961). Rate of penetration (ROP) is a complex variable that is a function of several parameters, including surface and downhole drilling parameters (Bingham 1965; Hareland and Rampersad 1994; Motahhari et al. 2010), drill bit and drilling fluid design (Durrand et al. 2010; Rahmani et al. 2021), drill bit wear state (Dupriest and Koederitz 2005), wellbore quality (Samuel et al. 2017), and rock properties (Bourgoyne Jr and Young Jr 1974; Kelessidis et al. 2015; Koulidis et al. 2021b).

Recent advances in machine learning and artificial intelligence have unlocked new technological innovations, gaining interest in the drilling industry (Zhong et al. 2022). Initially, the main focus was to detect and prevent unexpected events in the drilling process, including stuck pipe (Siruvuri et al. 2006; Miri et al. 2007) and associated challenges regarding drilling hydraulics (Ozbayoglu et al. 2002; Osman and Aggour 2003). Drilling hydraulics plays a critical role in the entire drilling process and involves a complex analysis to evaluate and predict the performance while drilling. Standpipe pressure prediction can provide an overview of the current condition of the wellbore (Todorov and Thonhauser 2014). Elkatatny et al. (2016) utilize an ANN model with 9000 drilling fluid field data, to predict rheological properties, including plastic viscosity, yield point and fluid density. Erge and van Oort (2022) developed a hybrid model to predict standpipe pressure during well construction using multiple sensor measurements. The results show an increase in the correlation coefficient to 0.9867 and a reduction of root-mean-square error (RMSE) by 22%.

Machine learning has started to be integrated into drilling optimization systems. Over the years, several models have been proposed to act as an advisory system and provide recommendations for the optimum drilling parameters, considering bit wear and real-time drilling data (Valisevich et al. 2015; Barbosa et al. 2019). The concept of mechanical specific energy (MSE) was introduced by Teale (1965) and built the foundation for addressing drilling optimization. Nautiyal and Mishra (2023) developed an ROP prediction model that utilizes ANN and random forest classifier by considering confined compressive strength (CCS), drill bit cutters, and drilling parameters. ANN has been used to evaluate the drilling performance for real-time operations. Hassan et al. (2020) utilized 20,000 actual drilling data to train seven ANN models and predict the drilling efficiency by coupling MSE and ROP. The results indicate that the developed ROP model provides a reliable prediction with an average absolute percentage error of 7.9%.

In the process of identifying the optimum optimization parameters, several more factors have to be considered. Drillstring vibrations are produced due to the forces acting on the drill bit while drilling and the contact of the drillstring with the wellbore (Sotomayor et al. 1997). An early investigation of surface measurements and analysis of drillstring vibrations was conducted by Macpherson et al. (1993). Their study provides insightful information regarding BHA dynamics modeling to identify the optimum operating conditions and shed light on the importance of real-time vibrations monitoring. Further development allowed the installation of the sub at any position in the drillstring (Deily et al. 1968). Currently, triaxial accelerometers are installed either on the surface or downhole (or at both locations) to acquire acceleration data in 3-axes (Xue et al. 2016). Drilling limiters are developed while drilling to consider the influence of the drilling action on wellbore quality (Kline et al. 2005; Dupriest et al. 2011).

This work utilizes the computed cutting forces obtained with in-cutter sensing technology to estimate the rock strength. An ANN model is utilized to predict the rock strength, rate of penetration and performance-scoring that is used to assess the drilling efficiency by considering vibration modes.

Methodology

Experimental setup and workflow

Machine learning is used to predict a variable and for the current case study rock strength, rate of penetration and performance-scoring. An extensive experimental study was performed using a scaled drilling rig to train the machine learning models. The scaled drilling rig is utilized to recreate the drilling process in the laboratory, but the main aim is to evaluate and utilize the cutter sensing technology. Safety limitations are applied as threshold values, including torque and axial force. Table 1 provides

Table 1 Scaled drilling rig operating limits

Parameter	Value	Unit
Rotary speed	0–1400	RPM
Drillstring buckling	580	N
Torque	0–7.2	Nm

information on some constraints of the scaled drilling rig. Safety factors are applied to each component, and in case the measured value reaches the drillstring buckling or torque limit, the motor that provides the axial displacement automatically stops.

The scaled drilling rig design allows a precise depth of cut control with an accuracy of ± 0.004 inches per foot. Data are transferred to LabVIEW using a data acquisition device (DAQ), serial interface, and on-screen buttons to control the setup and acquire the data. The instrumentation in the scaled drilling rig structure allows the acquisition of high-frequency sensor data, including rate of penetration, weight on bit, rotational speed, torque, force at the cutter, and vibrations. Details regarding the scaled drilling rig design, data acquisition and control system are discussed by Koulidis et al. (2021c). The workflow that describes the methodology of the current work is illustrated in Fig. 1.

In-cutter sensing

The two additional variables introduced and utilized in the current case study are in-cutter force sensing data and intrinsic specific energy (ε). Several experiments have been conducted with the in-cutter sensing and the results show a promising technology towards estimating the rock strength and cutter state while drilling (Koulidis et al. 2021c, 2022, 2023b)

The experiments were conducted in atmospheric conditions with controlled axial and rotational speed (0.2176 mm/s and 30 RPM, respectively). Figure 2 shows the placement of the miniature load cell behind the PDC cutter to measure the force perpendicular to cutter's face while drilling.

Samples of artificial gypsum are created with two layers of various mechanical properties. The test samples

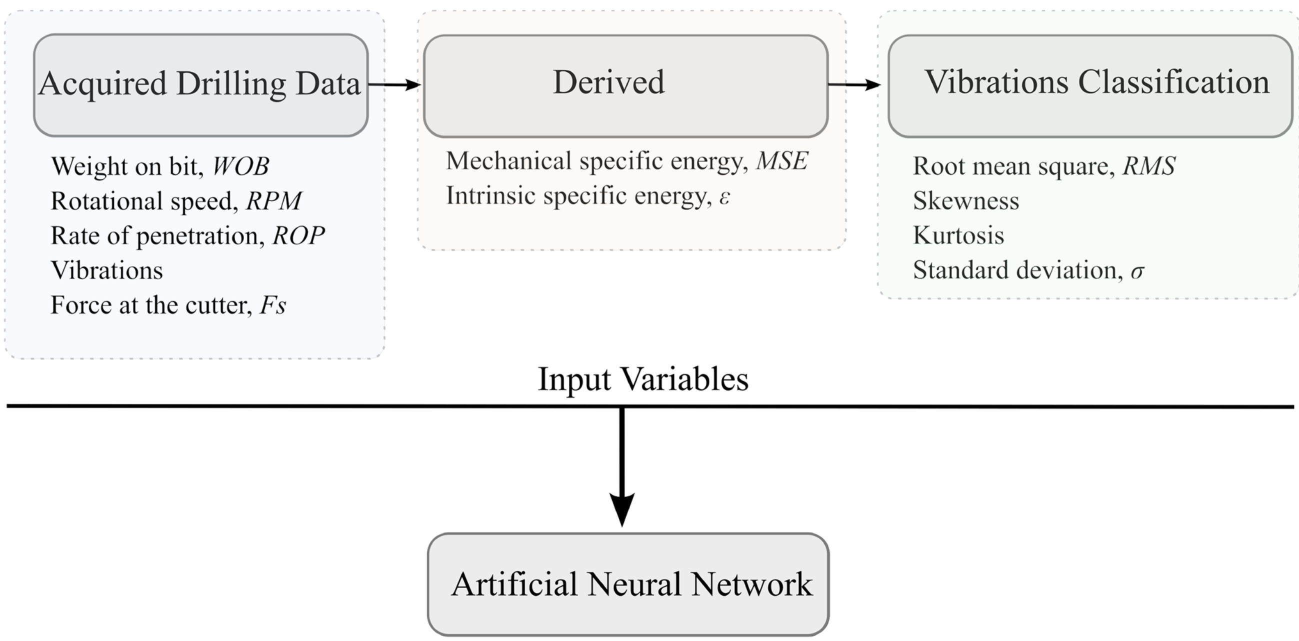

Fig. 1 Acquired data and derived parameters that are utilized as input variables for the ANN

Fig. 2 The scaled drill bit design that is utilized for the drilling tests

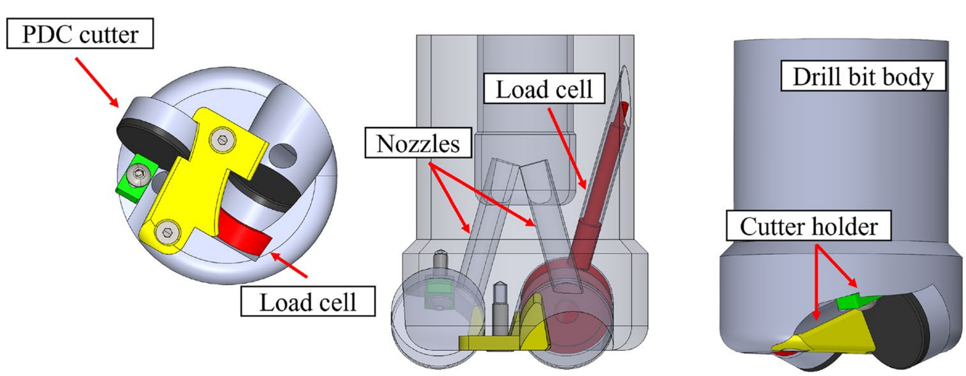

are drilled using random drilling parameters (WOB and RPM) for the preliminary testing in order to measure the corresponding MSE, force at the cutter, and vibrations. The mechanical oscillations of an object are referred to as vibrations. During the drilling process, due to the axial forces and rotation, different vibrations can be observed using accelerometers either downhole or at the surface (Koulidis et al. 2021a). To detect vibrations, an MPU9250 GYRO is installed close to the motor shaft, and Arduino Uno is used to collecting 3-axis accelerometer data in real-time. Manual classification is used to calculate the root mean square (RMS), skewness, kurtosis, and standard deviation to assess the vibration modes when off and on-bottom. Since there is no drilling activity, it is noted that the variances are minimal, particularly for RMS and standard deviation. However, the established measurements and the system's response to vibrations serve as the corresponding benchmark values.

Acquired experimental drilling data and vibrations classification

Since the formation tops are known, at the beginning of each formation, the axial and rotational speed are switched to 0.2176 mm/s and 30 RPM, to estimate the intrinsic specific energy (ϵ), which is correlated to the rock strength (Richard et al. 1998, 2012). The artificial gypsum samples are considered homogeneous and isotropic; thus, the intrinsic specific energy is estimated only at the beginning of the rock sample, and the average value is assumed for the remaining part of the layer. Figure 3 illustrates the acquired data and derived parameters from a drilling test that contains two rock layers. The data are utilized in the depth domain but, for more convenient illustration, are in the time domain. It is observed that the vibrations in X and Y direction are affected accordingly depending on the operating parameters. Naturally, the vibrations levels observed in the scaled drilling rig experiments are significantly lower compared to the ones observed during the actual drilling process. It is important to state that any mechanical equipment have limitations such as maximum torque limit or vibrations; thus, physical constrains are essential to evaluate the process.

To reliably assess the acquired vibration data, the sampling frequency should be substantially higher to capture even the transition between two rock samples. The synchronization between the two acquisition systems is accomplished by saving the data with a timestamp from both devices. Figure 4 provides an overview of the vibrations on X, Y and Z axis while rotating off bottom for different rotational speeds. For the acquired vibration data in Fig. 4, the corresponding RMS (root mean square), skewness, kurtosis, and standard deviation, as Fig. 5 illustrates. For the Y axis, the initial 9.8 g is due to gravity acceleration.

Each formation is drilled with a range of weight on bit, rotational and axial speed to create a dataset library for offline analysis. The data are then analyzed, classified, and prepared to be utilized as input to train the ANN model. Classifying the vibrations requires observing specific intervals while drilling, as shown in Fig. 6. The vibration mode (low, medium, and high) varies from off-bottom and depends on the drilling conditions for a particular formation. RMS and standard deviation are the primary two characteristics that distinguish between the vibration modes. The ranges for standard deviation are the following: 0–0.05 g corresponds to low vibration mode, 0.05–0.07 is medium, and greater than 0.07 is high, respectiv ely.

Artificial neural network (ANN)

Employed ANN maps the non-linear relationship of the inputs and corresponding outputs. All machine learning models are trained on the platform of MATLAB. The implemented ANN consists of three layers (input, hidden, and output) connected by weights and biases. Each layer is assigned with an activation function to introduce the nonlinearity. The coupled-training validation process is evaluated by their metric parameters, including relative mean square error (RMSE), average absolute percentage error (AAPE) and correlation coefficient (Tariq et al. 2022). Figure 7 illustrates the ANN architecture and workflow that is used to predict ROP.

The Levenberg-Marquardt method is used in the backpropagation of the training process. This method bypasses the need to compute the Hessian matrix and is one of the fastest algorithms in supervised learning problems using small- and moderate-sized ANNs. One-hot encoding is utilized to classify low, medium and high vibration modes. Since the ML output is data dependent, the most common comparison tool is the RMSE, as Eq. 1 shows (Tariq et al. 2022):

$$RMSE = \sqrt{\frac{1}{n}\sum_{i=1}^{n}(x_{exp} - x_{est})^2} \tag{1}$$

where x_{exp} is the expected and x_{est} is the estimated/predicted value. In addition, the average percentage relative error shows the difference of the expected to the estimated value as per Eq. 2 (Tariq et al. 2022):

$$AAPE = \frac{100}{n}\sum_{i=1}^{n}\left|\frac{x_{exp} - x_{est}}{x_{est}}\right| \tag{2}$$

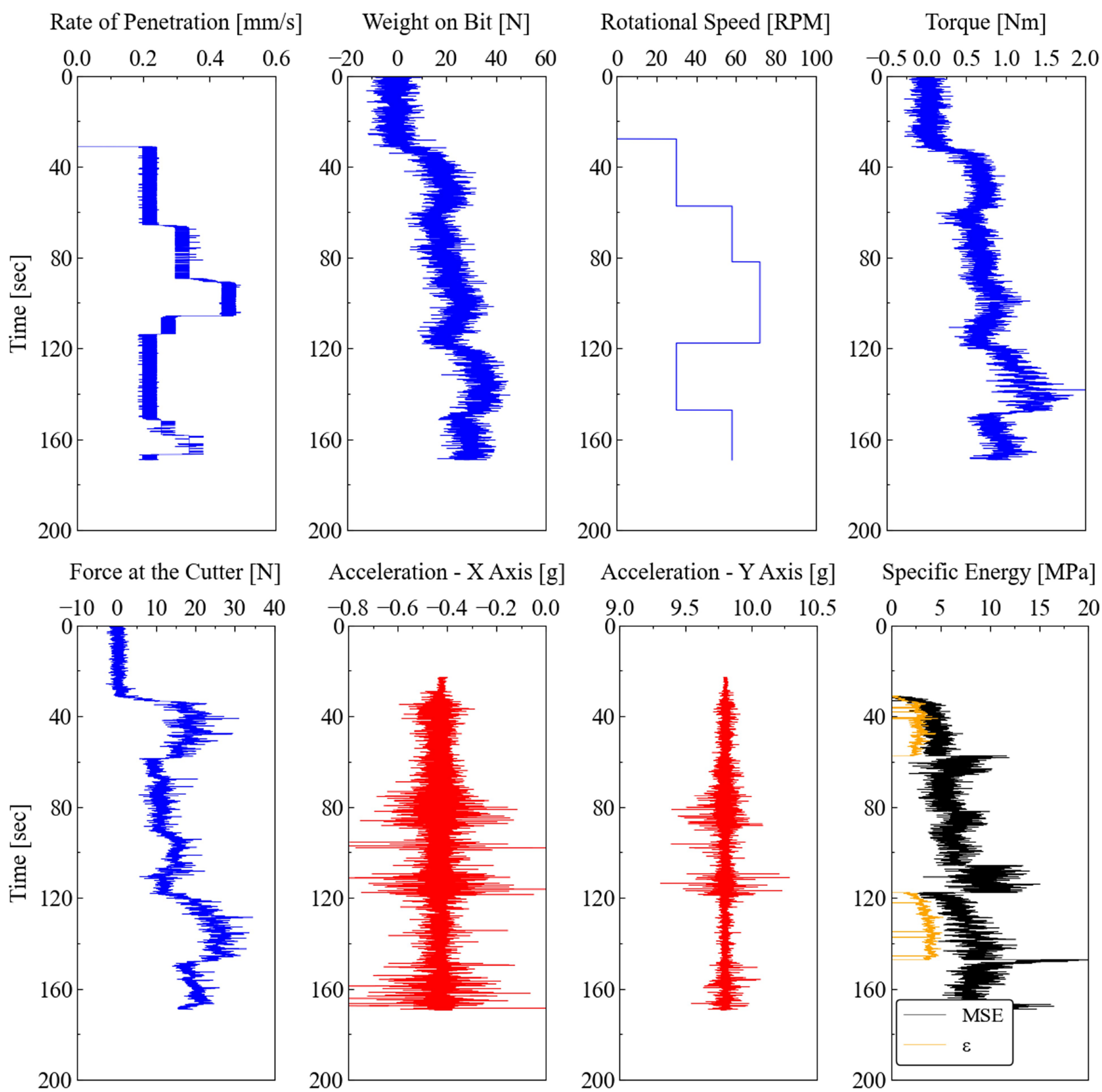

Fig. 3 Acquired data and derived variables from a single test. The footage drilled is approximately 40 mm

Rate of penetration and scoring prediction for single rock

Grid search optimization of neural network hyperparameters

This section details the optimization of the number of layers of the ANN and the number of neurons in each layer via the grid search method (Liashchynskyi and Liashchynskyi 2019; Erdogan Erten et al. 2021). In many machine learning problems, shallow ANNs lack the capability to learn higher-order features, while deeper ANNs suffer from vanishing and exploding gradients. On the other hand, including excessive amounts of neurons in an ANN result in unnecessary memory and computational costs (Hu et al. 2016). The grid search method allows a complete analysis of selected ANN hyperparameters over the search space within predefined boundaries and suitable grid resolutions (Bengio 2012). Since the dimensions of the input and output data in this study are relatively small, the grid search method can be completed within a reasonable amount of time. Based on the number of inputs, the search is conducted on a grid

Fig. 4 Example of vibrations data for different rotational speeds (off-bottom). The data are separated per applied rotational

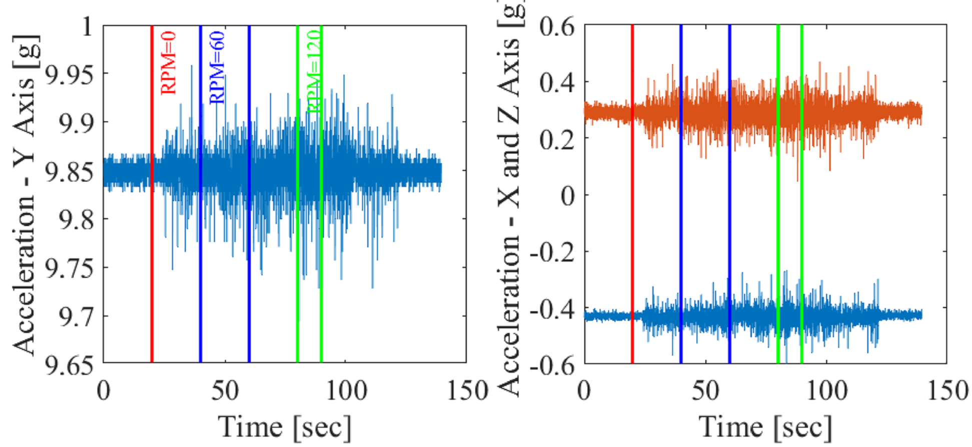

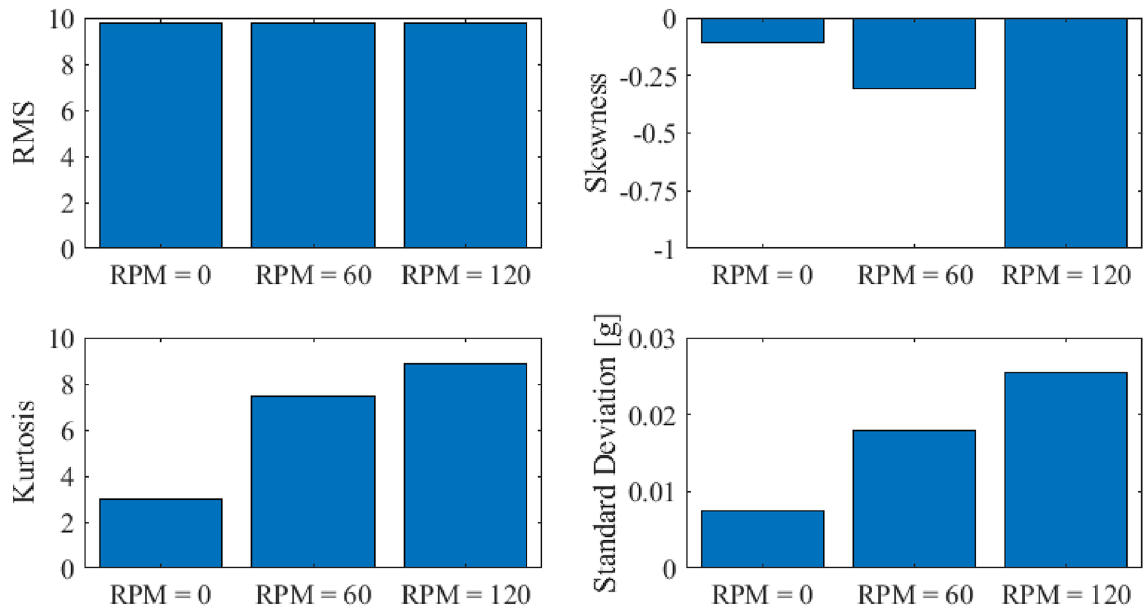

Fig. 5 Vibration's interpretation to analyze low, medium and high modes while rotating off bottom

constructed by varying the hyperparameters, as shown in Table 2.

The ANNs constructed according to the hyperparameters on the grid points are trained with the same dataset that feed 1×10 vectors to the input layer and corresponds to a single float value ROP label. From the search, the optimal values for the number of layers and neurons are 1 and 15, respectively. The resulting mean absolute errors (MAEs) (Reich et al. 2016) are shown in Fig. 8.

Scoring

It was stated in the introduction section that wellbore quality could significantly be decreased during high-vibration modes. Even though the drilled intervals for the current tests are approximately 40 mm, the effect of vibrations cannot be generalized and evaluated. Thus, it is important to implement this reaction as part of the drilling efficiency. The classified vibration modes are low, medium and high, corresponding to 1, 0.5 and 0.01 respectively. In the actual drilling process, excessive vibrations significantly increase the surface MSE, which impacts the drilling efficiency. The following Fig. 9 provides vibration data from a deviated well (16A (78)-32) located in Utah (Gilmour et al. 2021). As the drillstring oscillates in higher frequency, it has a low effect on the downhole MSE, since it is near to the drill bit, but higher peaks on the surface MSE as it is observed at approximately 6245 ft (Koulidis et al. 2023a).

For the current case, the weight coefficient of the vibrations with respect to ROP is 0.6. The weight coefficient is an

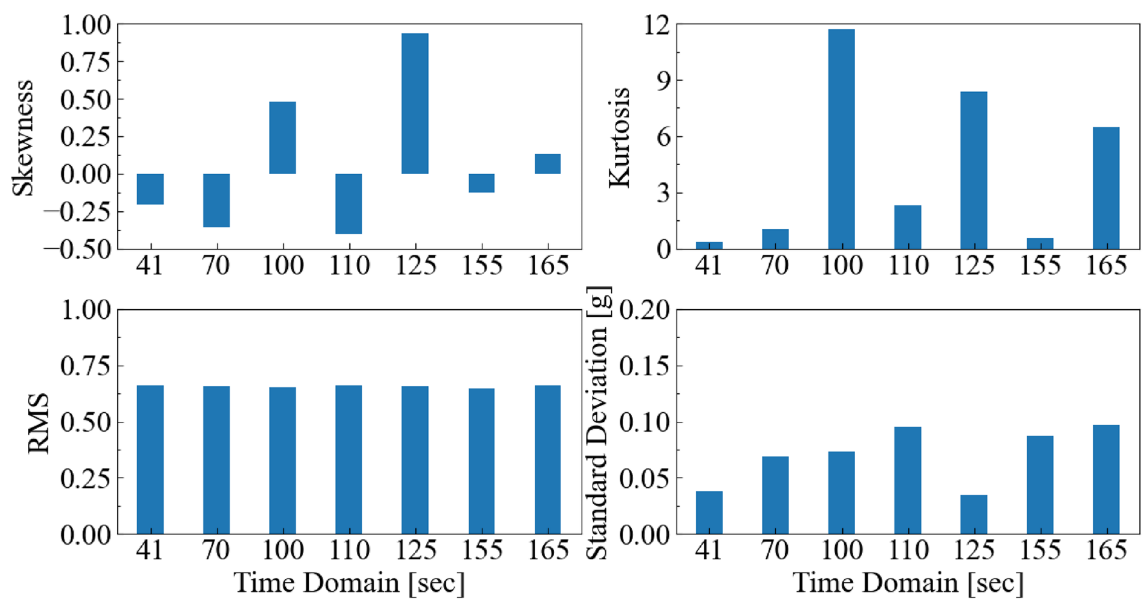

Fig. 6 Vibration's interpretation to analyze low, medium and high modes while drilling

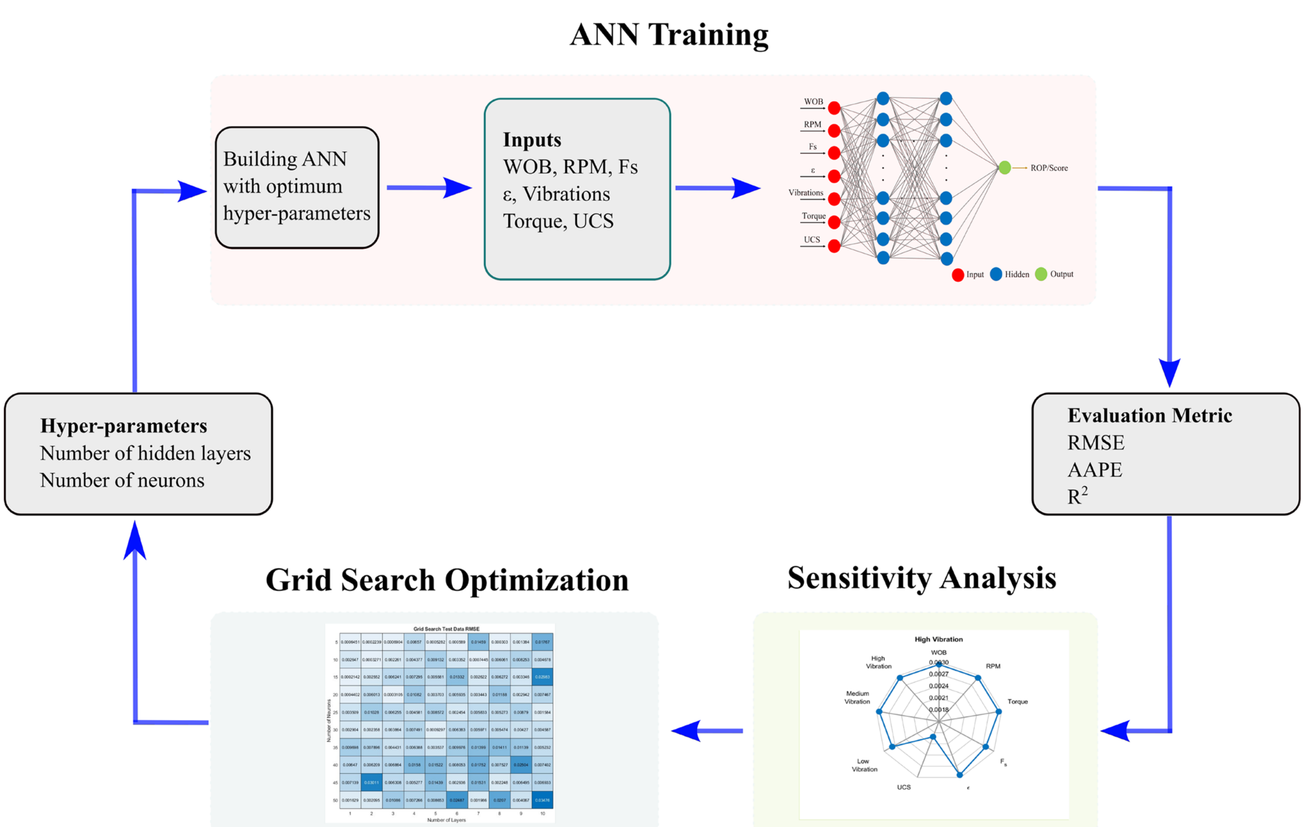

Fig. 7 ANN architecture and workflow

Table 2 Grid search hyperparameter properties

Hyperparameter	Star value	Step size	End value
Neurons per layer	5	5	50
Number of layers	1	1	10

empirical value that is selected to demonstrate the importance of coupling the vibrations with MSE; thus, the optimum segregation value is the 0.6 for our dataset to capture the behavior and to distinguish efficient and insufficient drilling process. The normalized MSE and score are calculated as per Eqs. 3 and 4.

$$MSE_{Normalized} = \frac{MSE - MSE_{min}}{MSE_{max} - MSE_{min}} \tag{3}$$

$$Score = MSE_{Normalized} + VibrationsScore_{Normalized} * Coefficient \tag{4}$$

Sensitivity analysis

An exhaustive sensitivity analysis has been conducted on the input data to evaluate the importance of each attribute in training the ANN (Szecówka et al. 2011). Although numerous methods in the literature reduce the dimensions of data and provide lower computational costs, such as the principal component analysis (Hameed et al. 2021) and the Monte Carlo method (Guevara et al. 2015) and, the relatively small input size of this study allows the complete search for optimal feature combinations. The features are combined into nCr arrangements, where n represents the total number of attributes and r = 1, 2, ..., n. From the results, the combination that provides the lowest RMSE is WOB, RPM, Torque,

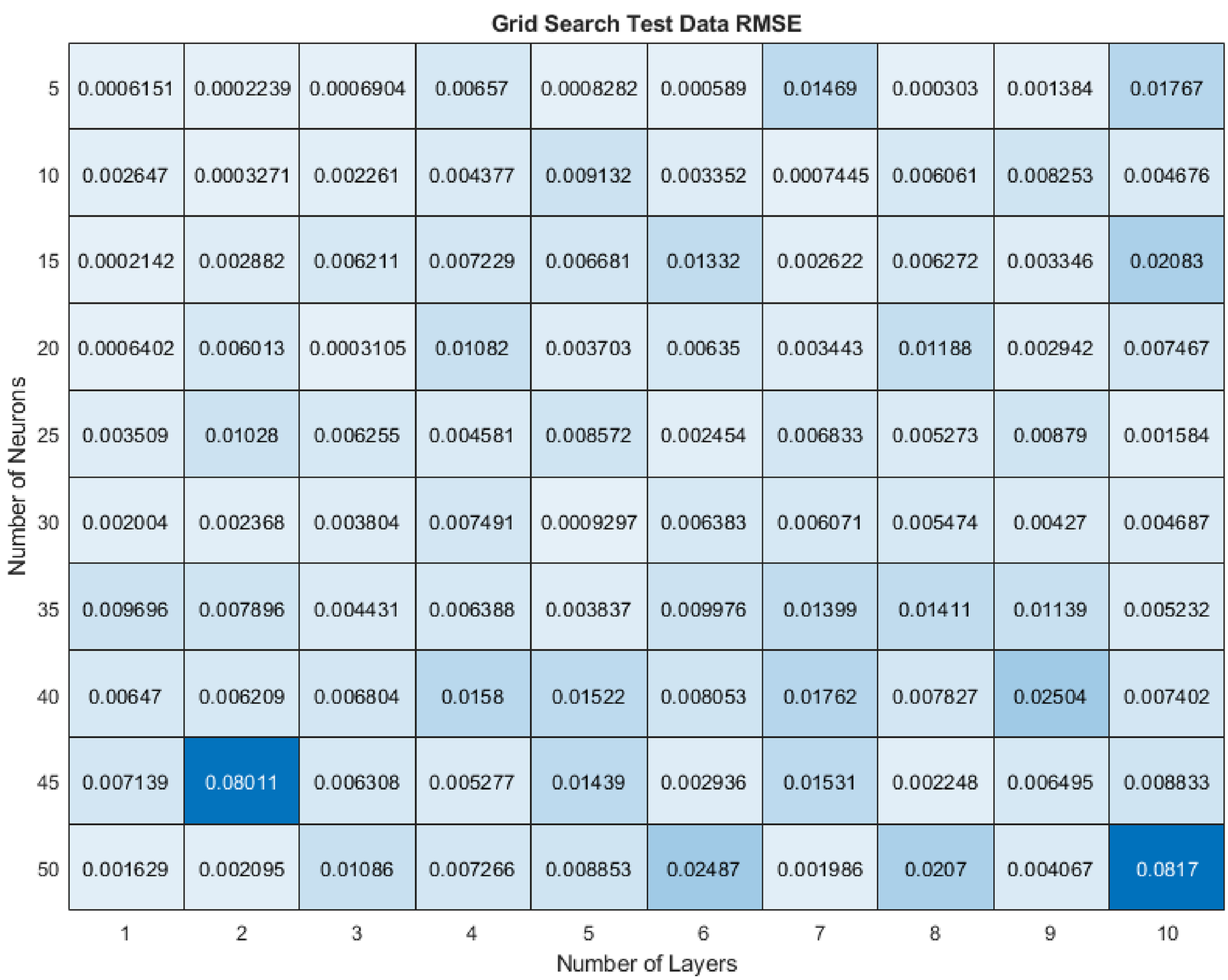

Fig. 8 Heatmap of the grid search test data root mean square errors (RMSEs)

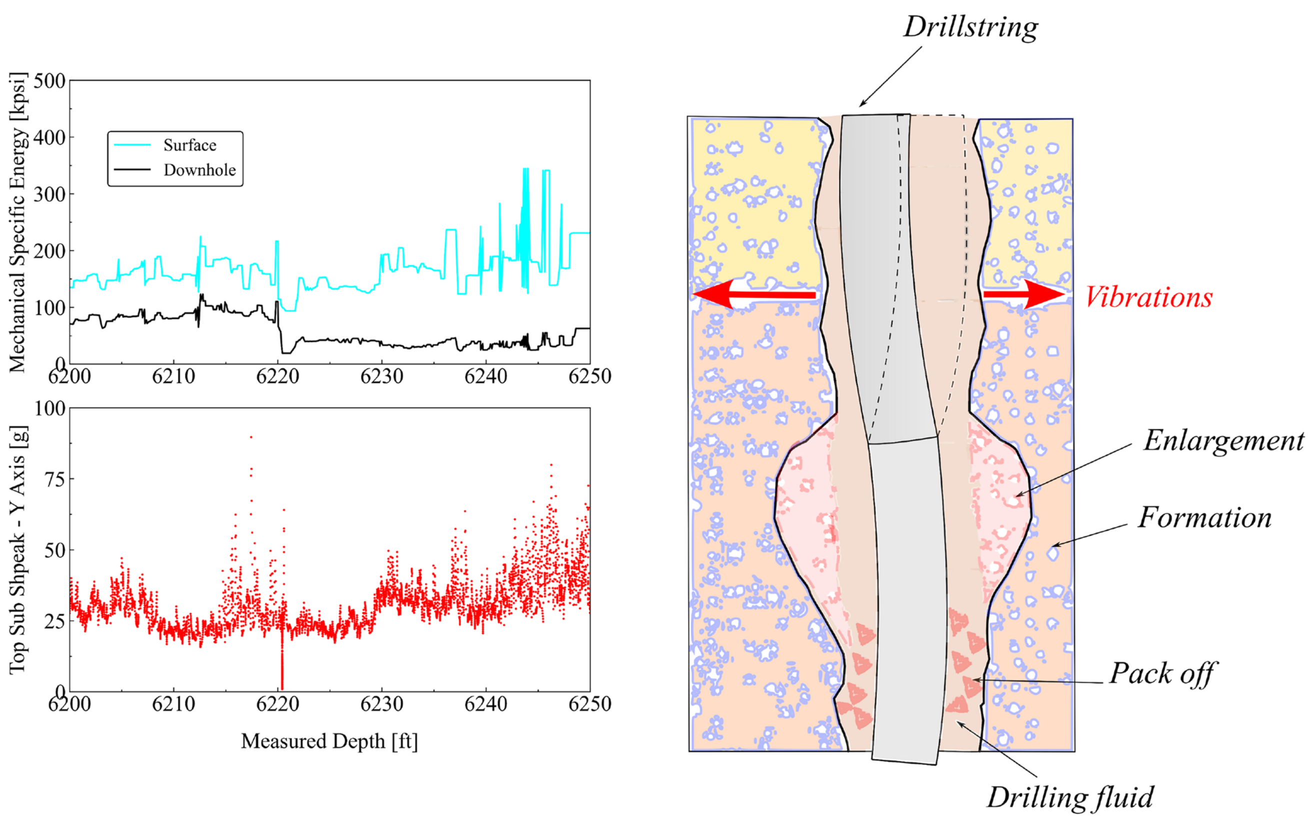

Fig. 9 (Left) Surface and downhole MSE, (Right) Schematic illustrating the effect of vibrations. Excessive vibrations result in an increase of contact of the drillstring with the wellbore

Fs, MSE, low vibration, medium vibration, and high vibration. The importance of each attribute is investigated with identical sensitivity analysis that is implemented for the scoring as Fig. 10 illustrates.

Results

Two layer rate of penetration prediction

The experiments were separated into different subsets depending on the drilling parameters vibrations, with 70% of the data to be used for training, 15% for testing and 15% for validation. Figure 11 illustrates the corresponding predicted rate of penetration by utilizing the Levenberg–Marquardt (LM) training algorithm.

The rate of penetration has significantly high variations in actual drilling applications due to the drilling action that produces vibrations. As it is observed in Fig. 3, the ROP shows a discrete behavior since the DC motor provides an accurate rotational speed (which is converted to axial). During the drilling of two rock layers (Fig. 3), different vibrations modes are observed that are produced from different rotational and axial speeds (ROP). Figure 11 provide the training and testing data sets, with the results showing accurate and reliable ROP prediction for two different layers.

In addition, several outliers are observed during the transition between two different ROP intervals. The R^2 for training and testing is 0.988 and 0.993, accordingly.

Two layer scoring prediction

From an operational perspective, predicting the score can provide significant insights regarding the drilling process, and this can be implemented in drilling operations where vibrations significantly impact the drilling process and wellbore quality. Figure 12 provides insights regarding the predicted score for drilling two rock samples with different parameters. The scoring procedure can be used as an advisory system regarding MSE and vibrations. For the current study, scoring below 0.6 represents low drilling efficiency.

Compared to the rate of penetration prediction, the AAPE is significantly higher. Outliers on the training and the testing dataset are observed, affecting the prediction model, and increasing the residual error. The following Fig. 13

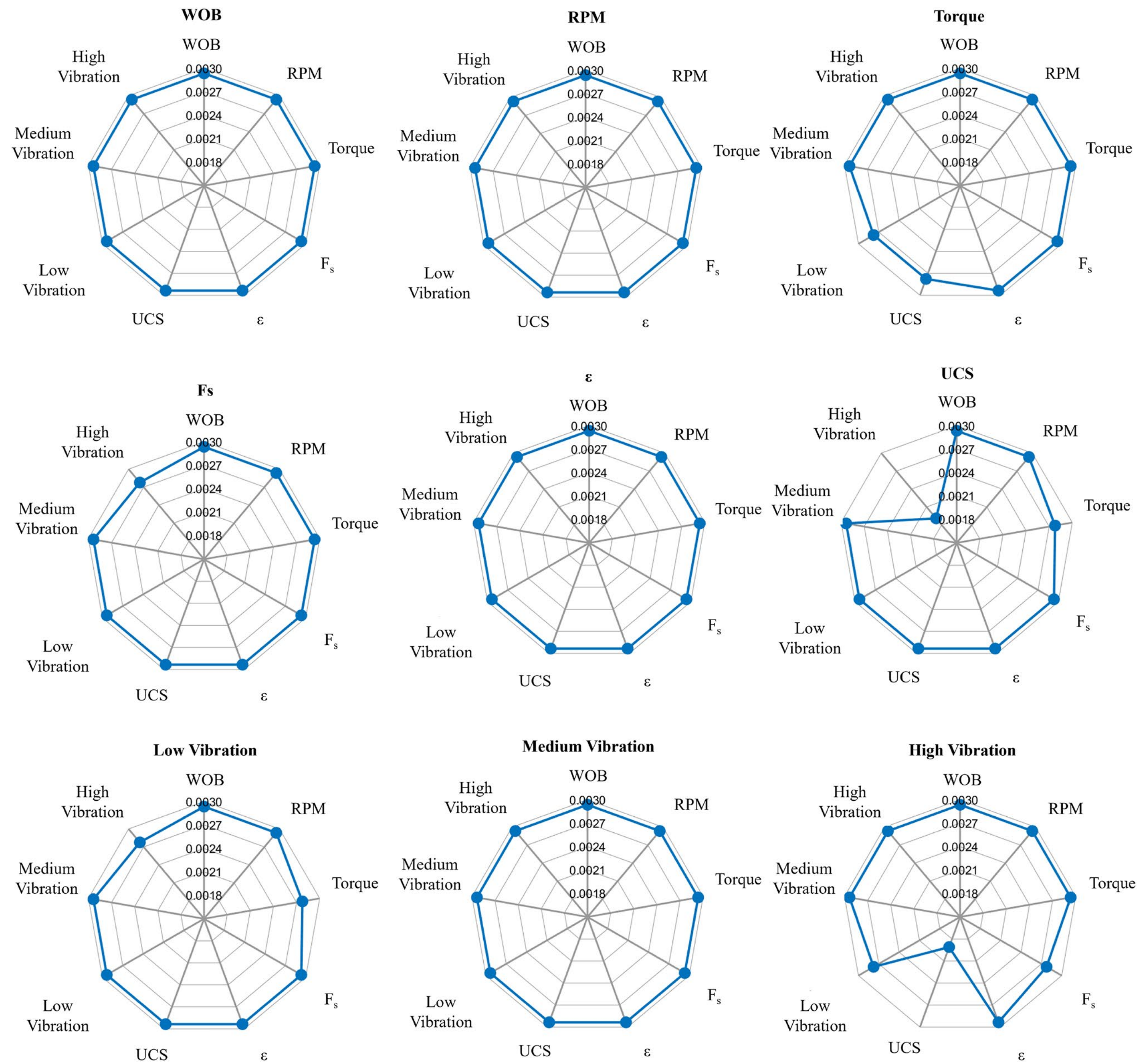

Fig. 10 Maximum RMSE per attribute visualized on a spider plot

visualizes the distribution of the residual error, which is close to the mean value for training and testing.

Interestingly, the scoring can be evaluated and assessed as quick visualization regarding the drilling efficiency while drilling (Fig. 14). The effect of the vibrations on MSE can be captured and utilized as a drilling efficiency indicator while drilling different rock layers. From a practical aspect, scoring intervals with a value below 0.6 represent the decreased rate of penetration, increased MSE and increased vibration.

Multiple layer rock strength prediction

For the training process we used the dataset of 8 samples and the 9th sample is an unseen layer. Figure 15 shows that utilizing the input data to train the model that contains great variations of the intrinsic specific energy (which is correlated with the rock strength), significantly assists in predicting the intrinsic specific energy (ε) for the unseen rock layer. The results show an excellent match with the actual intrinsic specific energy.

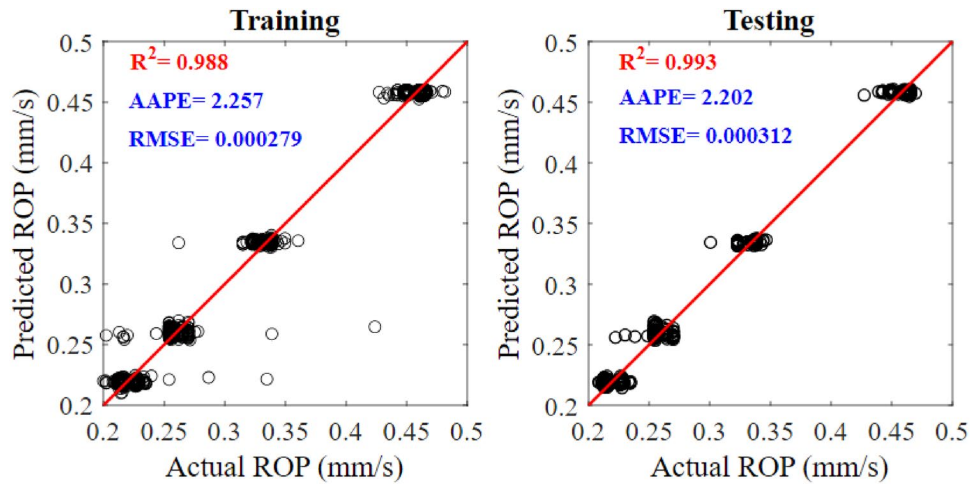

Fig. 11 Training and tested datasets and the corresponding R^2 and AAPE

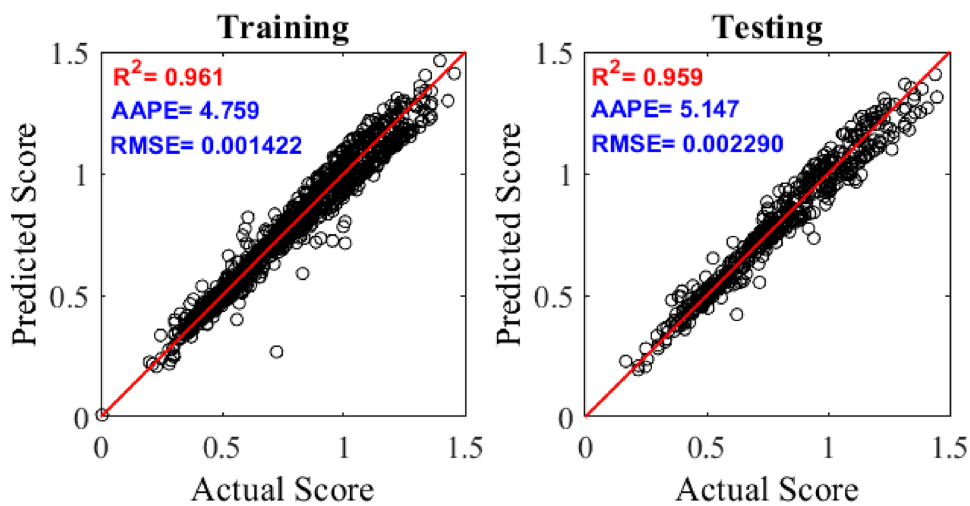

Fig. 12 Training and tested datasets and the corresponding R^2 and AAPE

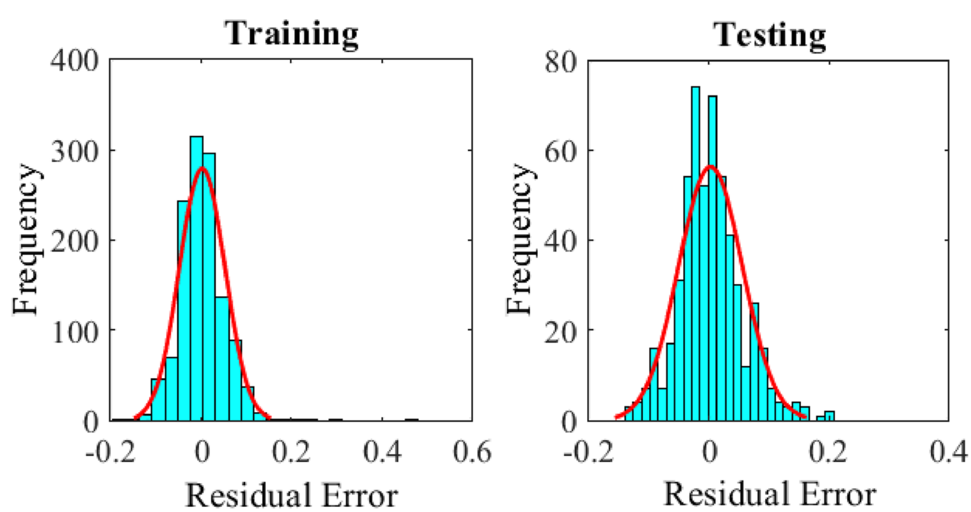

Fig. 13 Residual error for the training and testing datasets

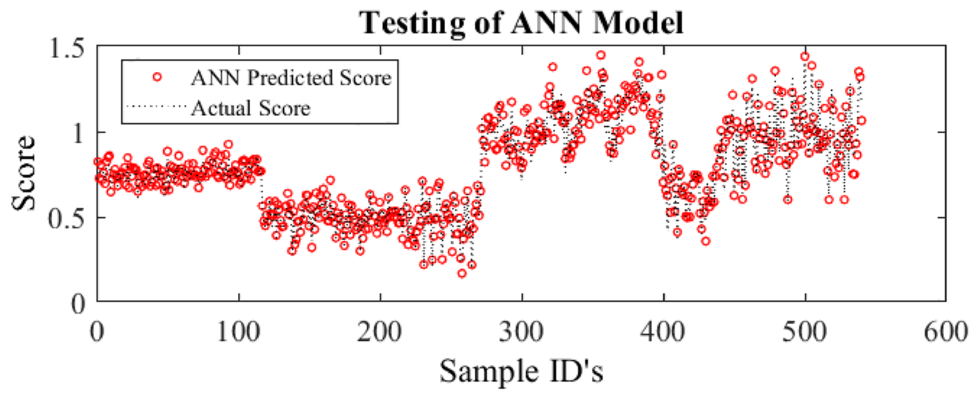

Fig. 14 Predicted and actual score for the two layers drilled

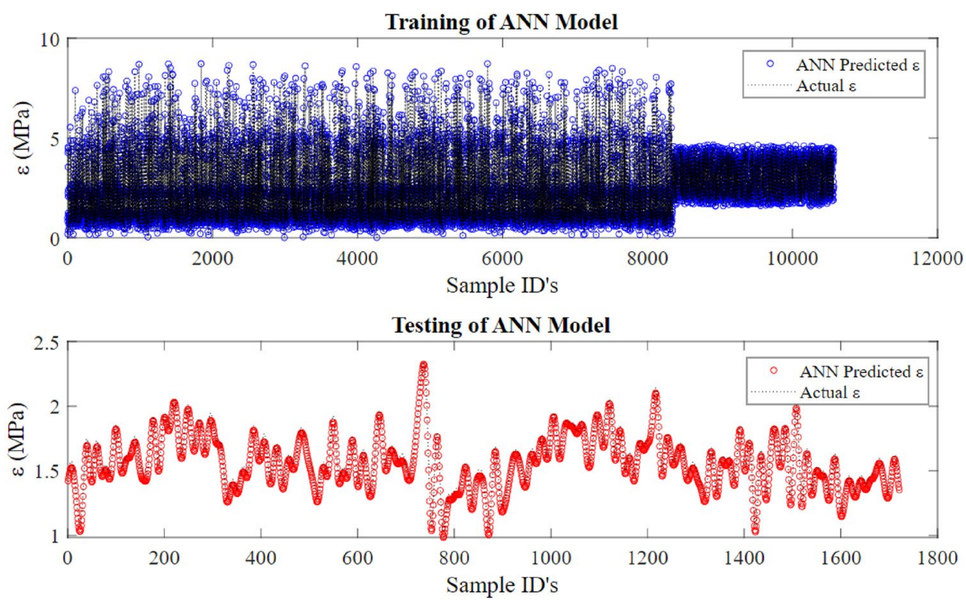

Fig. 15 Training and testing results with the suggested ANN model

Compared with the previous methodology to predict rock strength, all the acquired data are utilized for training the ANN model. The unseen rock layer is a formation that has a uniaxial compressive strength of approximately 1.7 MPa. The rate of penetration and rotational speed are analogous to the trained dataset but WOB, torque and intrinsic specific energy significantly differ.

Multiple layer scoring prediction

Even though the scoring prediction is feasible for two layers, the great challenge remains in predicting after drilling multiple layers. In total, five tests (two-layer samples) are performed that contain rock samples with a rock strength from 2.5 MPa to approximately 10 MPa. Four rock samples have similar rock strength, but the applied drilling parameters during the test varied. For each drilling test, one-hot encoding is performed to classify the vibration modes and estimate the intrinsic specific energy to obtain the rock strength. Figure 16 shows that utilizing the input data to train the model that contains great variations of the mechanical specific energy significantly assists in predicting the scoring.

The scoring mechanism provides a rapid visualization regarding the drilling efficiency, as Fig. 17 illustrates. The score can instantly change by reducing the rotational speed. This can be observed at approximately 3000 data points (Fig. 17), in which while drilling a rock of 10 MPa, by reducing rotational speed, the vibration mode changes from high to low; thus, the score increases. Overall, in several intervals, the drilling efficiency is significantly low, but it is important to state that the output is purely case-dependent in this stage. The same formations might be drilled more efficiently if the machine's mechanical limitations are greater, or the drill bit design differs. Thus, the resulted score only indicates the efficiency for the current scaled drilling rig.

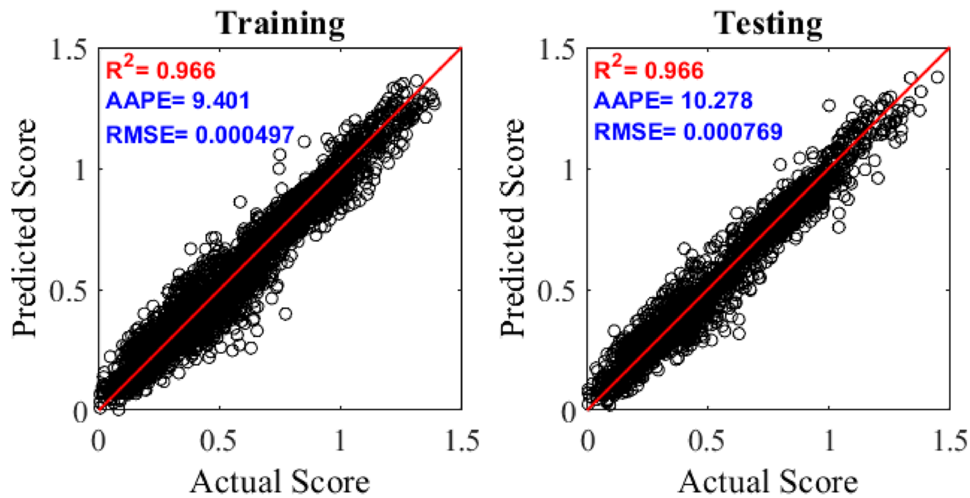

Fig. 16 Predicted and actual score for a combined dataset of five tests

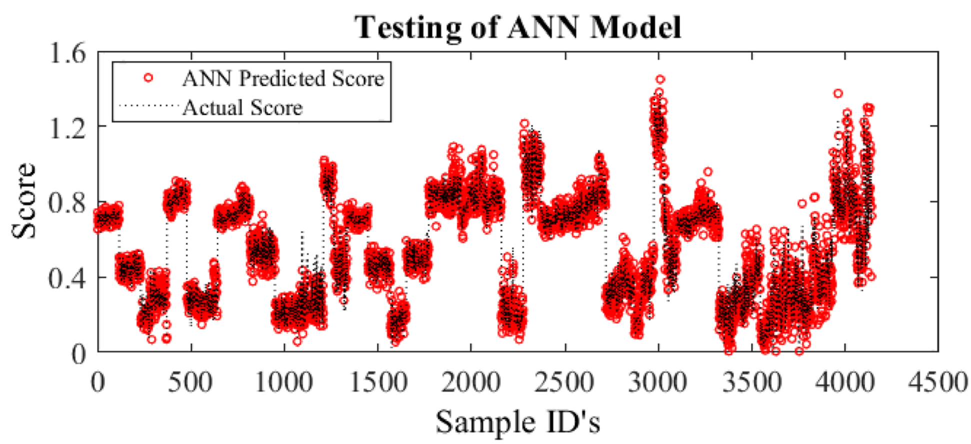

Fig. 17 Predicted score is excellently matched with the actual score

Discussion

The foundations of implementing the ANN model with in-cutter sensing and vibration data have already been established, but additional elements must be considered for an actual field application. The current methodology utilizes artificial gypsum samples where the mechanical properties can be controlled depending on the gypsum-to-water ratio and curing period. The rock strength can be accurately estimated and predicted for a new unseen layer for the same axial and rotational speed (0.2175 mm/s and 30 RPM). This corresponds to the major implementation of in-cutter sensing, which allows us to compute the rock strength while drilling. The main restriction of a scaled drilling rig is the output power, and due to the rotational cutting action of the drill bit, torque is the primary limiting variable. It is observed that during the experimental drilling tests, the variability of the measured forces is induced due to several factors, including [1] the brittle nature of the rock-cutting process, [2] axial and rotational movement, and [3] heterogeneities in the gypsum samples. To assess rock samples with higher rock strength, the drillstring rotational speed has to be increased to reduce the instantaneous depth of the cut.

The optimum depth of cut to achieve ductile failure and determine the rock strength is a function of the rock's mechanical characteristics. In the lab, each cutter's instantaneous depth of cut can be computed accurately, with the design providing an accuracy of ± 0.004 inches per foot. Actual drill bits are complex mechanical designs, with the cutting area of several cutters to intercept. The main attribute, the depth of cut, is very challenging to compute with accuracy while using surface measurements and a drillstring that is extended for several kilometers. Several technological advancements show the industry's interest and capabilities to invent technologies specified to the cutter scale, including shaped-cutter technology (Shao et al. 2022), rolling PDC cutter (Giumelli et al. 2014), and drill bits with incorporated depth of cut control (Alkhazal et al. Alkhazal et al. 2022).

In-bit sensing and subs are well-established technologies that are currently utilized (Sugiura 2008; Sugiura and Jones 2019; Kouzaiha et al. 2022). The main benefit of switching from a cutter scale to a drill bit scale is the integration of downhole sensors either on the drill bit body or a sub. Some of these bit-subs can provide feedback on torsional, lateral, and axial vibrations to the surface and detect severe downhole conditions. Integrating in-cutter and in-bit sensing can unlock the full potential of downhole data and predict the drilling efficiency with the current methodology.

The concept behind the proposed system is based on knowledge of the rock strength while drilling. The advisory system should utilize the acquired data and conduct the AI-based solution to evaluate the drilling efficiency and optimize the drilling process.

Conclusions

This work extended the drilling experiments to approximately 40 mm of drilled footage. Installing the vibration sensors allows for conducting a more comprehensive analysis of the drilling process and the applied drilling parameters. We introduced a novel framework that integrates AI and in-cutter sensing to enhance the prediction of rock strength and the drilling efficiency (scoring), providing a rapid and robust method to identify the optimum drilling parameters concerning physics constraints. Salient conclusions follow:

1. The rock strength can be accurately predicted for a new unseen layer for the same axial and rotational speed, 0.2175 mm/s and 30 RPM.
2. The in-cutter force sensing measurements allow monitoring of the forces acting on a single PDC cutter, which corresponds to a better prediction of the rock strength and is associated with a decrease in absolute error.
3. The ANN could be successfully implemented to predict the rock strength with the same accuracy that it was estimated by utilizing analytical modelling.
4. Statistical analysis demonstrates that the best performance occurred with 1 hidden layer and 15 neurons.
5. The ANN achieved an accuracy comparable to analytical modelling using less variables as input while operating in real-time.
6. It is shown via iterative permutations that rock strength and modes of vibration are crucial measurements for the prediction of ROP.
7. Ultimately, the score prediction could provide insight into the drilling efficiency, and its implementation allows quick visualization and evaluation of the drilling operation.
8. To provide a scoring concerning the drilling process, grid-search optimization is deployed to determine the optimum hyperparameters of ANN. In addition, a comprehensive sensitivity analysis is performed to evaluate each parameter's influence on ANN.
9. The results show that the ANN model accurately predicts training and testing datasets for scoring while drilling a single layer.

Acknowledgements The authors would like to express gratitude to King Abdullah University of Science and Technology for funding and supporting this work. Also, the authors would like to thank Dr. Zeeshan Tariq and Dr. Xupeng He for their assistance in providing insightful knowledge regarding machine learning.

Funding Alexis Koulidis was funded by the King Abdullah University of Science and Technology (KAUST) through baseline research funds to Prof. Shehab Ahmed.

Declarations

Conflict of interest The authors declare that they have no conflict of interest.

References

Alkhazal SA, Mahdi MJ, Barrera JLQ, Aljishi M (2022) improving drilling efficiency through heterogeneous formations and reduce stick slip levels after the implementation of self-adjust depth of cut technology in oil well. In: Abu Dhabi international petroleum exhibition and conference. SPE-211503-MS. https://doi.org/10.2118/211503-MS

Barbosa LFF, Nascimento A, Mathias MH, de Carvalho JA Jr (2019) Machine learning methods applied to drilling rate of penetration prediction and optimization—a review. J Pet Sci Eng 183:106332. https://doi.org/10.1016/j.petrol.2019.106332

Bengio Y (2012) Practical recommendations for gradient-based training of deep architectures. In: Neural networks: tricks of the trade: second edition. Springer, Berlin, pp 437–478

Bingham MG (1965) A new approach to interpreting–rock drillability

Bourgoyne AT Jr, Young F Jr (1974) A multiple regression approach to optimal drilling and abnormal pressure detection. Soc Petrol Eng J 14(04):371–384. https://doi.org/10.2118/4238-PA

Deily FH, Dareing DW, Paff GH, Ortloff JE, Lynn RD (1968) Downhole measurements of drill string forces and motions. J Eng Ind 90(2):217–225. https://doi.org/10.1115/1.3604617

Dupriest FE, Koederitz WL (2005) Maximizing drill rates with real-time surveillance of mechanical specific energy. In: SPE/IADC drilling conference and exhibition. SPE-92194-MS. https://doi.org/10.2118/92194-MS

Dupriest FE, Elks WC, Ottesen S, Pastusek PE, Zook JR, Aphale CR (2011) Borehole-quality design and practices to maximize drill-rate performance. SPE Drill Complet 26(02):303–316. https://doi.org/10.2118/134580-PA

Durrand C, Skeem M, Hall D (2010) Thick PDC, shaped cutters for geothermal drilling: a fixed cutter solution for a roller cone drilling environment. In: ARMA US rock mechanics/geomechanics symposium. ARMA-10-524

Elkatatny S, Tariq Z, Mahmoud M (2016) Real time prediction of drilling fluid rheological properties using artificial neural networks visible mathematical model (white box). J Petrol Sci Eng 146:1202–1210. https://doi.org/10.1016/j.petrol.2016.08.021

Erdogan Erten G, Bozkurt Keser S, Yavuz M (2021) Grid search optimised artificial neural network for open stope stability prediction. Int J Min Reclam Environ 35(8):600–617. https://doi.org/10.1080/17480930.2021.1899404

Erge O, van Oort E (2022) Combining physics-based and data-driven modeling in well construction: hybrid fluid dynamics modeling. J Nat Gas Sci Eng 97:104348. https://doi.org/10.1016/j.jngse.2021.104348

Gilmour B, Wooden J, Pulka F, Rose B, Barker C, Borchardt E (2021) Utah forge: well 16a(78)-32 logs. https://doi.org/10.15121/1777912

Giumelli M, O'Shea P, Maliardi A, Sosnowski P, Shepherd A, Sadawarte SS, Scordella M (2014) Offshore exploration program benefits from rolling PDC cutter technology, timor sea Australia. In: IADC/SPE Asia Pacific drilling technology conference and exhibition. SPE-170532-MS. https://doi.org/10.2118/170532-MS

Guevara I, Gutierrez M, Zuniga P (2015) Identification of weak buses for proper placement of reactive compensation through sensitivity analysis using a neural network surrogate model. In: 2015 IEEE international autumn meeting on power, electronics and computing (ROPEC). https://doi.org/10.1109/ROPEC.2015.7395084

Hameed MM, AlOmar MK, Baniya WJ, AlSaadi MA (2021) Incorporation of artificial neural network with principal component analysis and cross-validation technique to predict high-performance concrete compressive strength. Asian J Civ Eng 22:1019–1031. https://doi.org/10.1007/s42107-021-00362-3

Hareland G, Rampersad PR (1994) Drag—bit model including wear. In: SPE Latin America/Caribbean petroleum engineering conference. SPE-26957-MS. https://doi.org/10.2118/26957-MS

Hassan A, Elkatatny S, Al-Majed A (2020) Coupling rate of penetration and mechanical specific energy to improve the efficiency of drilling gas wells. J Nat Gas Sci Eng 83:103558

Hu H, Peng R, Tai YW, Tang CK (2016) Network trimming: a data-driven neuron pruning approach towards efficient deep architectures. arXiv:1607.03250

Kelessidis VC, Ahmed S, Koulidis A (2015) An improved drilling simulator for operations, research and training. In: SPE middle east oil and gas show and conference. SPE-172793-MS. https://doi.org/10.2118/172793-MS

Kline WE, Chandler K, Keller SR, Ottesen S, Gupta V, Tenny M (2005) Physics-based well design—beyond the learning curve. In: IPTC international petroleum technology conference. IPTC-10709-MS. https://doi.org/10.2523/IPTC-10709-MS

Koulidis A, Abdullatif M, Abdel-Kader AG, Ayachi Mi, Ahmed S, Gooneratne C, Magana-Mora A, Affleck M, et al (2021a) Field assessment of camera based drilling dynamics. In: SPE middle east oil and gas show and conference. SPE-204634-MS. https://doi.org/10.2118/204634-MS

Koulidis A, Kelessidis V, Ahmed S (2021b) Exploitation of field drilling data with an innovative drilling simulator: highly effective simulation of rotating and sliding mode. In: SPE/IADC middle east drilling technology conference and exhibition. SPE-202176-MS. https://doi.org/10.2118/202176-MS

Koulidis A, Mohamed F, Ahmed S (2021c) Micromechanics of drilling: a laboratory investigation of formation evaluation at the bit. In: SPE middle east oil and gas show and conference. SPE-204670-MS. https://doi.org/10.2118/204670-MS

Koulidis A, Zhan G, Ahmed S (2022) Embedded force sensing at the cutter. In: Abu Dhabi international petroleum exhibition & conference. SPE-211511-MS. https://doi.org/10.2118/211511-MS

Koulidis A, Abdullatif M, Ahmed S (2023a) Drilling monitoring system: mud motor condition and performance evaluation. In: SPE middle east oil and gas show and conference. SPE-213422-MS. https://doi.org/10.2118/213422-MS

Koulidis A, Pelfrene G, Ahmed S (2023b) Experimental investigation of the rock cutting process and derivation of the 3d spatial distribution of the formation strength using in-cutter sensing. J Pet Explor Prod Technol 14:365–380. https://doi.org/10.1007/s13202-023-01712-4

Kouzaiha R, Sayyaleh S, Khalil A, Borayek A, Reyad M, Al Otaibi A (2022) Using in-bit data capturing sensors to identify and reduce dysfunctions using a higher drilling efficiency shaped cutter solution. In: Abu Dhabi International petroleum exhibition and conference. SPE-213645-MS. https://doi.org/10.2118/211535-MS

Liashchynskyi P, Liashchynskyi P (2019) Grid search, random search, genetic algorithm: a big comparison for NAS. https://doi.org/10.48550/arXiv.1912.06059

Macpherson JD, Mason JS, Kingman JEE (1993). Surface measurement and analysis of drillstring vibrations while drilling. https://doi.org/10.2118/25777-MS

Miri R, Sampaio J, Afshar M, Lourenco A (2007) Development of artificial neural networks to predict differential pipe sticking in Iranian offshore oil fields. In: SPE international oil conference and exhibition in Mexico. SPE-108500-MS

Motahhari HR, Hareland G, James J (2010) Improved drilling efficiency technique using integrated PDM and PDC bit parameters. J Can Pet Technol 49(10):45–52. https://doi.org/10.2118/141651-PA

Nautiyal A, Mishra AK (2023) Machine learning application in enhancing drilling performance. Procedia Comput Sci 218:877–886

Osman E, Aggour M (2003) Determination of drilling mud density change with pressure and temperature made simple and accurate by ann. OnePetro. In: Middle east oil show. SPE-81422-MS

Ozbayoglu EM, Miska SZ, Reed T, Takach N (2002) Analysis of bed height in horizontal and highly-inclined wellbores by using artificial neural networks. In: SPE international thermal operations and heavy oil symposium. SPE-78939-MS

Rahmani R, Pastusek P, Yun G, Roberts T (2021) Investigation of PDC cutter structural integrity in hard rocks. SPE Drill Completion 36(01):11–28

Reich NG, Lessler J, Sakrejda K, Lauer SA, Iamsirithaworn S, Cummings DA (2016) Case study in evaluating time series prediction models using the relative mean absolute error. Am Stat 70(3):285–292. https://doi.org/10.1080/00031305.2016.1148631

Richard T, Detournay E, Drescher A, Nicodeme P, Fourmaintraux D (1998) The scratch test as a means to measure strength of sedimentary rocks. In: SPE/ISRM rock mechanics in petroleum engineering. SPE-47196-MS. https://doi.org/10.2118/47196-MS

Richard T, Dagrain F, Poyol E, Detournay E (2012) Rock strength determination from scratch tests. Eng Geol 147:91–100. https://doi.org/10.1016/j.enggeo.2012.07.011

Samuel GR, Azar JJ, Aideyan P (2017) Applied drilling engineering optimization. Sigmaquadrant Engineering Publication, Houston
Shao F, Liu W, Gao D, Zhao X (2022) Development and verification of triple-ridge-shaped cutter for PDC bits. SPE J 27(06):3849–3863. https://doi.org/10.2118/210580-PA
Siruvuri C, Nagarakanti S, Samuel R (2006) Stuck pipe prediction and avoidance: a convolutional neural network approach. In: IADC/SPE drilling conference. SPE-98378-MS
Sotomayor GP, Placido JC, Cunha J (1997). Drill string vibration: how to identify and suppress. https://doi.org/10.2118/39002-MS
Speer JW (1959) A method for determining optimum drilling techniques. In: SPE upper gulf coast drilling and production conference. SPE-1242-MS. https://doi.org/10.2118/1242-G
Sugiura J (2008) The use of the near-bit vibration sensor while drilling leads to optimized rotary-steerable drilling in push- and point-the-bit configurations. In: SPE Asia Pacific oil and gas conference and exhibition. SPE-115572-MS. https://doi.org/10.2118/115572-MS
Sugiura J, Jones S (2019) A drill bit and a drilling motor with embedded high-frequency (1600 Hz) drilling dynamics sensors provide new insights into challenging downhole drilling conditions. SPE Drill Complet 34(03):223–247. https://doi.org/10.2118/194138-PA
Szecówka P, Szczurek A, Licznerski B (2011) On reliability of neural network sensitivity analysis applied for sensor array optimization. Sens Actuat B Chem 157(1):298–303
Tariq Z, Murtaza M, Mahmoud M, Aljawad MS, Kamal MS (2022) Machine learning approach to predict the dynamic linear swelling of shales treated with different waterbased drilling fluids. Fuel 315:123282
Teale R (1965) The concept of specific energy in rock drilling. Int J Rock Mech Min Sci Geomech Abstr 2(1):57–73
Todorov D, Thonhauser G (2014) Hydraulic monitoring and well control event detection using model based analysis. In: Offshore technology conference Asia. OTC-24803-MS. https://doi.org/10.4043/24803-MS
Valisevich A, Ruzhnikov A, Bebeshko I, Moreno R, Zhentichka M, Bits S (2015) Drillbit optimization system: real-time approach to enhance rate of penetration and bit wear monitoring. In: SPE Russian petroleum technology conference. SPE-176517-MS. https://doi.org/10.2118/176517-MS
Wardlaw H (1961) Simplified analysis aids in optimizing drilling factors for minimum cost. J Pet Technol 13(05):475–482
Xue Q, Leung H, Wang R, Liu B, Huang L, Guo S (2016) The chaotic dynamics of drilling. Nonlinear Dyn 83:2003–2018
Zhong R, Salehi C, Johnson R Jr (2022) Machine learning for drilling applications: a review. J Nat Gas Sci Eng 108:104807. https://doi.org/10.1016/j.jngse.2022.104807